

Low Mutual Coupling of Hexagonal Bar Slotted Dual-Band Four-Port MIMO Textile Antenna for WBAN and 5G Applications

1st Hamza A. Mashagba

Faculty of Electronic Engineering &
Technology Universiti Malaysia Perlis
(UniMAP), 02600 Arau, Perlis,
Malaysia

Centre of Excellence for Advanced
Communication Engineering (ACE),
Universiti Malaysia Perlis (UniMAP),
01000 Kangar, Perlis, Malaysia

Perlis, Malaysia

gasabhamz@gmail.com

2nd Hasliza A Rahim

Faculty of Electronic Engineering &
Technology Universiti Malaysia Perlis
(UniMAP), 02600 Arau, Perlis,
Malaysia

Centre of Excellence for Advanced
Communication Engineering (ACE),
Universiti Malaysia Perlis (UniMAP),
01000 Kangar, Perlis, Malaysia

Perlis, Malaysia

haslizarahim@unimap.edu.my

3rd Mohd Najib Mohd Yasin

Faculty of Electronic Engineering &
Technology Universiti Malaysia Perlis
(UniMAP), 02600 Arau, Perlis,
Malaysia

Centre of Excellence for Advanced
Communication Engineering (ACE),
Universiti Malaysia Perlis (UniMAP),
01000 Kangar, Perlis, Malaysia

Perlis, Malaysia

najibyasin@unimap.edu.my

4th Mohd Haizal Jamaluddin

Wireless Communication Centre,
Faculty of Electrical Engineering,
Universiti Teknologi Malaysia (UTM),
Johor Bharu, Malaysia

Johor Bharu, Malaysia

haizal@utm.my

5th Liyana Zahid

Faculty of Electronic Engineering &
Technology Universiti Malaysia Perlis
(UniMAP), 02600 Arau, Perlis,
Malaysia

Centre of Excellence for Advanced
Computing (AdvComp), Technology
Universiti Malaysia Perlis (UniMAP),
02600 Arau, Perlis, Malaysia

Perlis, Malaysia

liyanazahid@unimap.edu.my

6th Nur Hidayah Ramli

Faculty of Electronic Engineering &
Technology Universiti Malaysia Perlis
(UniMAP), 02600 Arau, Perlis,
Malaysia

Centre of Excellence for Advanced
Communication Engineering (ACE),
Universiti Malaysia Perlis (UniMAP),
01000 Kangar, Perlis, Malaysia

Perlis, Malaysia

hidayahramli@unimap.edu.my

7th Sarun Narongkul

Faculty of Industrial Technology,
Songkhla Rajabhat University,
Songkhla, Thailand
Songkhla, Thailand
sarun.ch@skru.ac.th

Abstract— The paper presents a methodology to reduce Mutual Coupling (MC) in a 4-port dual-band Multiple-Input-Multiple-Output (MIMO) textile antenna, specifically designed for biomedical applications. This antenna utilizes MIMO technology and operates within the Wireless Body Area Network (WBAN) and Fifth Generation (5G) across two distinct frequency bands: 2.45 GHz and 3.5 GHz. The structure comprises four octagonal patch antennas, each incorporating a bar and hexagonal slot, with individual patch dimensions of 48.5 x 30 mm². A hybrid approach to minimize MC is investigated for patches positioned at a proximity of 0.15 λ . The antenna is evaluated with bending conditions in different curvature angles to test its robustness in practical on-body. The antenna achieves the MC of -30 dB and a maximum realized gain of 2.42 dBi at the lower band and 5.6 dBi at the upper band. Notably, the antenna's performance exceeds the expected attenuation effects caused by the lossy nature of the human body, indicating a good agreement between the modeled and experimental results.

Keywords— Antennas, bioelectromagnetics, wearable antenna, MIMO antenna, mutual coupling reduction, wearable

I. INTRODUCTION

In wearable MIMO antennas, achieving compactness requires positioning multiple antenna elements nearby, which inherently leads to increased MC—a phenomenon negatively impacts antenna performance parameters, such as gain,

efficiency, and channel capacity. MC is a challenging issue in wearable applications, where the influence of the human body exacerbates these effects due to its lossy nature. To maintain optimal performance in such compact arrangements, various techniques for reducing MC have been proposed, including structural modifications such as adding slots [1], utilizing metamaterials [2], introducing parasitic elements [3], and employing neutralization lines [4]. Each of these methods has demonstrated effectiveness, but they often come with drawbacks such as increased design complexity or limitations in achieving a compact, textile-friendly structure.

Metamaterials have emerged as a popular solution due to their ability to manipulate electromagnetic waves, thus reducing interaction between closely spaced elements [2]. However, the incorporation of metamaterials can complicate the overall design, potentially making it less suitable for wearable applications that require flexibility and ease of integration. Parasitic elements and neutralization lines provide effective isolation but may result in a bulkier design, which is not ideal for textile-based applications [3]. Hybrid techniques that integrate multiple coupling reduction strategies have also been explored, demonstrating notable success in minimizing MC while retaining performance efficiency [5]. These techniques often involve combining structural modifications,

such as adding slots or rotating patch elements, to enhance isolation between antenna elements.

II. METHODOLOGY AND RESULTS

The proposed antenna is designed to operate in dual-band mode. The proposed antenna operates in dual-band mode at 2.45 GHz for WBAN and 3.5 GHz for 5G, using a felt textile substrate ($\epsilon_r = 1.44$, $\tan \delta = 0.044$, thickness = 3 mm) and ShieldIt Super electro-textile (conductivity = 1.18×10^5 S/m). The antenna features a hexagonal slot in the rectangular patch to broaden the upper band, with an overall size of 140×140 mm² ($1.4\lambda \times 1.4\lambda$ at 2.45 GHz). Feeding points are strategically placed for the MIMO configuration.

Figure 1 illustrates the evolution of the antenna design, progressing from a single-element structure to a two-element array and ultimately to a four-element MIMO configuration. Each component features its own port, enhancing dual-band performance for WBAN and 5G applications, as detailed in [6].

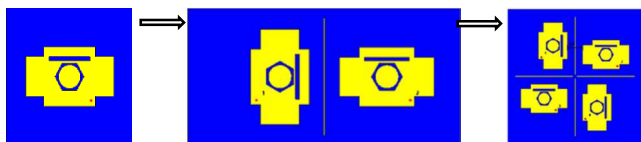


Fig. 1. Design evolution from single-element to four-element MIMO configuration for dual-band performance.

A. Hybrid Technique Analysis and S-Parameter Analysis of MIMO Configuration

Fig. 2 shows the Dimensions of the proposed Hexagonal Bar Slotted antenna. Fig. 3 shows the simulated result of S11 of the proposed hexagonal bar slotted antenna. The results show that the bandwidth is 6.3% and a maximum of up to 5.9% for lower and upper bands, respectively, at port 1. Fig. 3 also shows that the MC achieved less than -30 dB in both bands. Meanwhile, for the upper band, lower MC is obtained with $MC < -30$ dB for all ports of MIMO configurations.

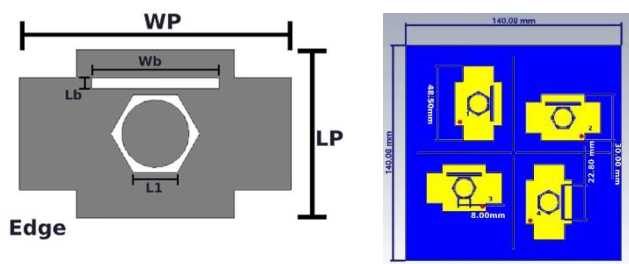


Fig. 2. Dimensions of proposed MIMO antenna design.

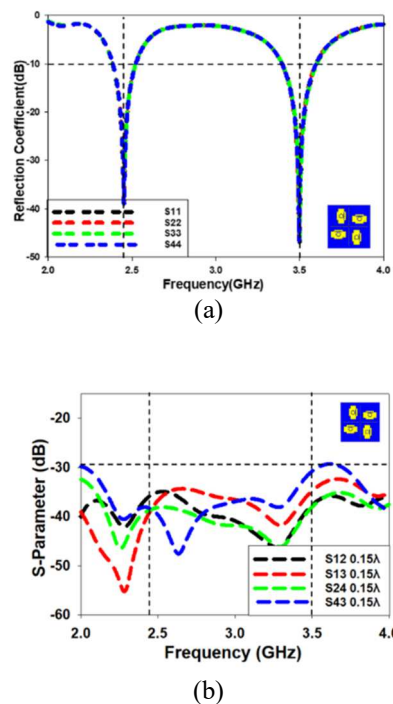


Fig. 3. Simulated results of the patch antenna gap 0.15λ with rotation and line patch (a) reflection coefficient Sii and (b) MC Sij.

B. Bending Evaluation

A comprehensive analysis on the effects of the bending on the proposed MIMO antenna is presented in this section. Simulations of the bending evaluation curvatures are formed at different angles (α) of 15° , 30° , 45° , 60° , and 90° , which translates to 534.69, 267.34, 178.23, 133.67, and 89.11 mm, radii at x-axis and y-axis, respectively, based on [5]. When wrapped around the arm in a regular body, these bending values are selected to emulate the curvature of the proposed MIMO antenna. Bending is investigated at two conditions when bent at x- and y-axes for six different bending angles, as illustrated in Fig. 4. Decreasing the bending degree from 60° to 15° lowers the resonance in both bands, with a more significant change in the upper band. In contrast, different MC behavior can be observed when bent at the x- and y-axes. When bent at the x-axis at 2.45 GHz, lower S21 is seen with increasing bending degrees. This behavior is contrary at 3.5 GHz. On the other hand, when varying the bending degree at the y-axis, the S21 fluctuates in the lower band but is almost consistent in the upper band. As expected, bending at an angle of 30° . The most critical scenario occurs when the antenna is bent at the y-axis with an angle/radius of $\alpha = 30^\circ @ 267.34$ mm, resulted in low MC at both frequency bands. Hence, it can be concluded that bending the antenna at different degrees particularly affected the performance at the higher frequencies.

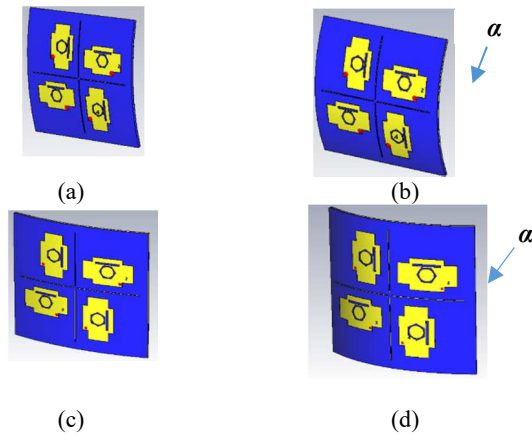


Fig. 4. The proposed MIMO with different bending angles: (a) bent at x-axis at 30°, (b) x-axis at 60°, (c) y-axis at 30° and (d) y-axis at 60°.

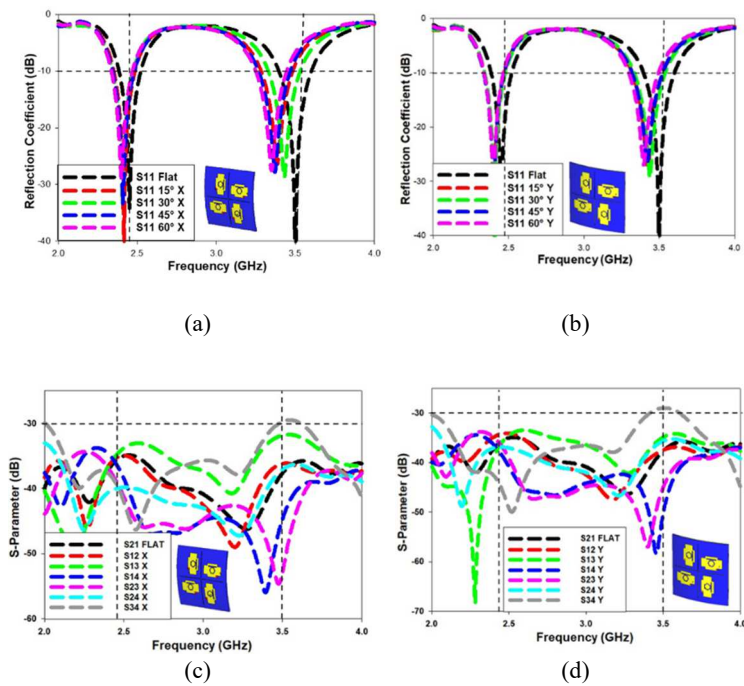


Fig. 5. Simulated results of the proposed MIMO antenna when bent at different angles: (a) S11 at x-axis and (b) S11 at y-axis (c) S21 at x-axis ($\alpha=30^\circ$) and (d) S21 at y-axis ($\alpha=30^\circ$).

The impact of bending on the antenna is more evident at higher frequencies compared to lower frequencies due to a combination of factors. First, higher frequencies have shorter wavelengths, making them more sensitive to physical changes such as bending. Even small variations in curvature can significantly alter resonant conditions at higher frequencies, leading to greater performance variations. Additionally, the electromagnetic fields at higher frequencies are more concentrated and closer to the surface of the antenna, making them more susceptible to the disturbances caused by bending. These changes affect the effective current distribution and electric fields more significantly. Lastly, the effective electrical length of the antenna is more severely altered at higher frequencies, which results in more noticeable resonance shifts compared to lower frequencies where such geometric changes have less impact.

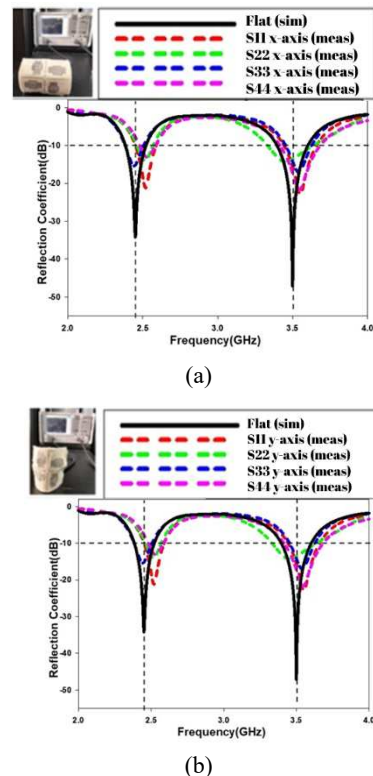
C. Experimental Evaluation

The fabricated MIMO antenna was tested experimentally in both a planar state and under bending conditions along both axes as shown in Fig. 6. Measurements were conducted using a Keysight Technologies E5071C E-series Vector Network Analyzer (VNA), with a 50- Ω coaxial cable connecting the SMA to the VNA for testing. The S11 and S21 results are shown in Fig. 7, where solid lines indicate the simulated performance, while dashed lines represent the measured results. The simulated S11 for the antenna in planar form closely matches the free-space measurements, as seen in Fig. 7 (a) and (b), with only a minor upward shift in the lower frequency band. The measured S11 for all bending configurations along the y-axis also shows good agreement, including similar bandwidths.

However, under extreme bending (30° along the y-axis), a downward shift in the lower band was observed. In the planar condition, the measured S21 is approximately -30 dB in both bands. When the antenna is bent along the y-axis, the measured S21 drops below -30 dB for all bending conditions in both the lower and upper bands. This suggests a significant reduction in MC under extreme bending, confirming the design's resilience to y-axis bending while retaining its dual-band performance.



Fig. 6. Photograph of the fabricated MIMO textile antenna (a) Front view and (b) back view.



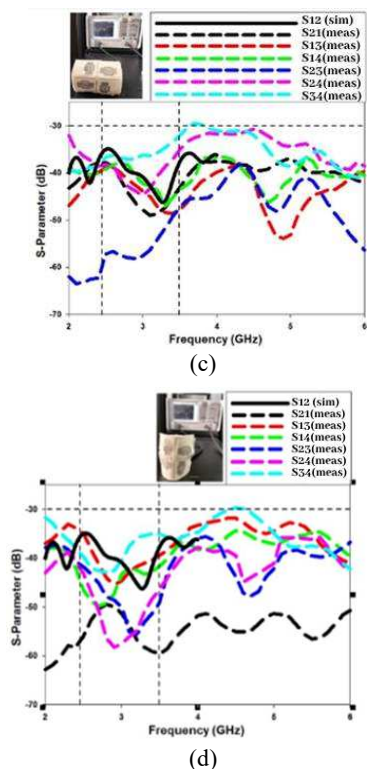


Fig. 7. Comparative analysis of simulated flat condition and measured S-parameters for the proposed MIMO antenna under the bending conditions at $\alpha=30^\circ$: (a) Sii with x-axis bending (b) Sii with y-axis bending, (c) Sij with x-axis bending and (d) Sij with y-axis bending.

D. SAR and On-Body Evaluations

The SAR distributions averaged over 10 g of tissue are then calculated at 2.45 GHz and 3.5 GHz for the two-port MIMO metamaterial antenna with an input power of 1 W when placed on chest. The SAR levels for this antenna in planar conditions indicate that the maximum 10 g SARs are observed to be 0.0963 W/kg at 2.45 GHz and 0.0113 W/kg at 3.5 GHz, respectively, as shown in Fig. 8. SAR distributions on average more than 10 g of tissue at frequencies of 2.4 & 3.5 GHz while taking an input power of 1 W into consideration. Fig. 9 shows good agreement between simulated results under flat and on-body condition (on chest) for both reflection coefficient and MC values (< -30 dB) across all ports.

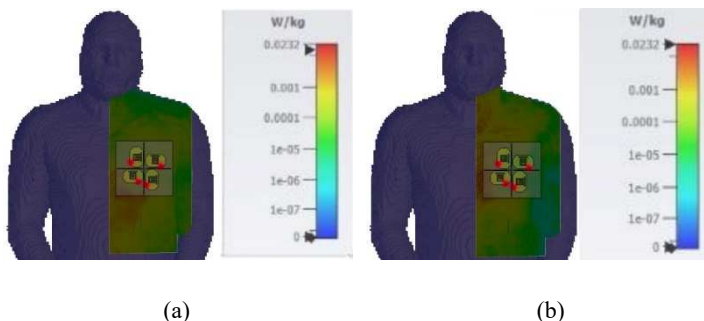


Fig. 8. SAR evaluation on Hugo body model at 10g on chest (a) 2.45 GHz and (b) 3.5 GHz.

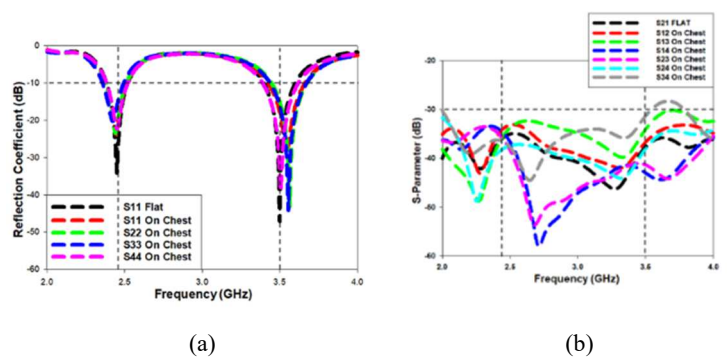


Fig. 9. On-body simulated results of the proposed MIMO (a) Sii antenna on the chest (b) Sij antenna on chest.

III. CONCLUSION

This study applies a hybrid approach to reduce MC in the design of a textile MIMO antenna for on-body and 5G applications. The antenna consists of four hexagonal structures, each integrated with a bar slot. MC is effectively minimized by rotating the patch elements and incorporating a line patch between the antenna elements. Notably, the optimized structure is simple and suitable for textile-based implementation. Evaluations of key MIMO parameters, including reflection coefficient, MC and realized gain, demonstrate that this antenna is well-suited for potential use in next-generation 5G wearable devices.

ACKNOWLEDGMENT

The authors would like to acknowledge the financial support under the INTERES grant from Songkhla Rajabhat University (SKRU) and KS Co. Ltd [grant no. 9008-00042]. KS Co. Ltd supports knowledge of the test and measurement for new technologies.

REFERENCES

- [1] M. Asif et al., "Design of a dual-band SNG metamaterial based antenna for LTE 4G/WLAN and Ka-band applications," *IEEE Access*, vol. 9, pp. 71553-71562, May 2021.
- [2] M. Nouri et al., "An optimized small compact rectangular antenna with meta-material based on fast multi-objective optimization for 5G mobile communication," *J. Comput. Electron.*, vol. 20, pp. 1532-1540, July 2021.
- [3] Y. Liu, Z. Yang, P. Chen, J. Xiao, and Q. Ye, "Isolation enhancement of a two-monopole MIMO antenna array with various parasitic elements for Sub-6 GHz applications," *Micromachines*, vol. 13, no. 12, Art. no. 2123, November 2022.
- [4] Vinoth and R. Vallikannu, "Design and analysis of metamaterial patch antenna 5G and X band applications," 2021 International Conference on Computer Communication and Informatics (ICCCI), Coimbatore, India, pp. 1-6, 2021.
- [5] H. A. Mashagba et al., "A hybrid mutual coupling reduction technique in a dual-band MIMO textile antenna for WBAN and 5G applications," *IEEE Access*, vol. 9, pp. 150768-150780, November 2021.
- [6] H. A. Mashagba et al., "Four-port dual-band textile MIMO antenna for biomedical health monitoring systems: on-body mutual coupling reduction characterization," *Physica Scripta*, vol. 99, no. 9, Art. no. 095026, August 2024.